Journal of Applied Polymer Science

Scaffolds Based on Hydroxypropyl Starch: Processing, Morphology, Characterization, and Biological Behavior

Itziar Silva,[1] Mariló Gurruchaga,[2] Isabel Goñi,[2] Mar Fernández-Gutiérrez,[1,3] Blanca Vázquez,[1,3] Julo San Román[1,3]

[1]Institute of Polymer Science and Technology, CSIC, C/Juan de la Cierva 3, Madrid 28006, Spain
[2]Department of Polymer Science and Technology, POLYMAT (Institute of Polymeric Materials), University of The Basque Country (UPV/EHU), San Sebastian 20080, Spain
[3]CIBER-BBN, Ebro River Campus, Building R&D, Poeta Mariano Esquillor s/n, Zaragoza 50017, Spain
Correspondence to: M. Gurruchaga (E-mail: marilo.gurruchaga@ehu.es)

ABSTRACT: In this study, a novel electrospun hybrid scaffold was developed, which consists of a blend of a modified natural substance, hydroxypropyl starch (HPS) with a synthetic one, poly(ethylene oxide) (PEO). Nanofibers with varying polysaccharide contents were fabricated using water as solvent and the electrospinning process conditions investigated as a function of the weight ratio of the blend. The fibers were characterized through mean diameter and morphology by scanning electron microscopy. Micrographs clearly showed the effect of HPS/PEO weight ratio of the blend on the nanofibers formation. Stability of the fibers was enhanced by coating with hydrophobic poly(methyl methacrylate) (PMMA). *In vitro* degradation analysis of the coated mats after 1 month of immersion showed porous formation, whereas the fibrous structure was retained. The biological response of the mats against human fibroblasts proved that cells were able to adhere to and proliferate on the fibrous materials. Thus, the feasibility of producing nanofibers of HPS/PEO blends with high proportion of starch and their biocompatibility after coating with PMMA was demonstrated, indicating that these materials have potential to be used as scaffolds in tissue engineering applications. © 2012 Wiley Periodicals, Inc. J. Appl. Polym. Sci. 000: 000–000, 2012

KEYWORDS: electrospinning; hybrid scaffolds; hydroxypropyl starch; biocompatibility; biomaterials; tissue engineering

Received 13 October 2010; accepted 22 February 2012; published online
DOI: 10.1002/app.37551

INTRODUCTION

The requirements for the design and production of an ideal scaffold are very complex and not yet fully understood. An ideal scaffold must be biocompatible both in bulk and degraded form, exhibit a porous, interconnected, and permeable structure to permit the ingress of cells and nutrients while also offering an appropriate surface structure and chemistry to enable enhanced cell adhesion and proliferation. Several techniques aim to produce a scaffold which can mimic, in some way, the architecture of the natural extracellular matrix (ECM). One of these techniques that has attracted a great deal of attention in the last few years is electrospinning.[1]

Electrospinning is considered to be a versatile and cost-efficient technique for producing multifunctional nanofibers from various polymers, such as polymer blends, composites, sol-gels, and ceramics.[2,3] Electrospun nanofibers have remarkable characteristics such as large surface-to-volume ratio and pore sizes in the nanorange.[3] These nanofibers form scaffolds of natural or synthetic polymers with a nonwoven porous structure that have already been used in tissue engineering applications, exhibiting excellent cell adhesion and proliferation.[4–6] Because of their unique properties such as the multifunctionality of nanofibers, flexibility in the selection of materials as well as the ability to control the scaffold's properties, electrospun scaffolds have already been used in vascular, bone, neural, and tendon/ligament tissue applications among others.[1,7–9]

Given that different cells have different needs, the ability to tailor porosity would be of great advantage and could in many cases be determinant in failure or success.[10] Pore size has also been seen to affect cell development when it comes to differentiation and matrix production.[11–13] The size range of nanofibers also offers interesting possibilities.

ECM separates different tissues, forms a supportive meshwork around cells, and provides anchorage to the cells. It is made up of proteins such as collagen and carbohydrate biopolymers such

as glycosaminoglycans (GAGs). For this reason, the electrospun scaffolds are often made of degradable polymers, such as collagen, chitosan, and gelatine, which are designed to degrade slowly in the body, disappearing as the cells begin to regenerate.[14–16] However, natural materials often lack the desired physical properties or are difficult to electrospin on their own, which has led to the development of hybrid systems, which consist of a blend of synthetic and natural materials.[1,14]

There are many hybrid systems described in the literature, it is common to encounter scaffolds composed of chitosan and poly (ethylene oxide) (PEO),[17] gelatine, and poly(L-lactide-*co*-ε-caprolactone) (PLCL),[18] as well as those combining synthetic materials with natural proteins to overcome shortfalls observed when using scaffolds constructed with any natural substance on its own for example collagen/elastin/poly(caprolactone) (PCL),[14] collagen/glycosaminglycan[11] or bombyx mori silk/PEO[19] among others.

The number of recent studies regarding electrospun polysaccharides and their derivatives, which are potentially useful for regenerative medicine, has increased dramatically. Among the critical challenges facing electrospun polysaccharide nanofibers, we could emphasize: the appropriate selection of the polysaccharide, the synthesis of its various derivatives, the use of mixed solvents, the use of hybrids of natural and/or synthetic polymers, the fabrication of core–shell structures, blowing-assisted electrospinning, and the fabrication of micro/nanofiber composites. Typically used polysaccharides are alginate, cellulose, chitin, chitosan, hyaluronic acid, starch, dextran, and heparin. While most of these polysaccharides are of potential interest for electrospinning and have been found to be useful in many biomedical applications, there are still limitations to be overcome in electrospinning. In addition, difficulties regarding the processability of the polysaccharides, e.g., poor solubility in organic solvents and high surface tension, have limited their application so far.[20–23] A variety of approaches have been reported to improve solubility including the synthesis of derivatives and the use of mixed solvent systems. High viscosity caused by inherently high molecular weights and electrical charge also produced poor electrospinnability of some polysaccharides. These shortfalls can be overcome by varying the blend ratio with other polymers or by varying the composition of the solvent.[24]

Among the natural polymers, starch is one of the most commonly used in the field of biomaterials because of its biodegradability, biocompatibility, abundance in nature and low cost. On the other hand, its main drawback is how difficult it is to electrospin. It is difficult to find articles describing the use of starch in electrospinning processes because of the many problems it gives. There are only a few references which describe scaffolds obtained with 30% starch using the electrospinning process. These scaffolds were obtained either by blending the 30% starch with PCL,[25–29] nanofibers with poly(vinyl alcohol) (PVA)/cationic starch[30] or using starch acetate on its own.[31]

For all of the aforementioned, in this study a novel electrospun hybrid scaffold is developed, consisting of a blend of a modified natural material, in this case hydroxypropyl starch (HPS) with a synthetic one, in this case PEO. PEO was selected as the polymer additive to produce electrospun nanofibers because of its biocompatibility and ability to form fibers with the aim of producing a suitable scaffold for biomedical applications such as tissue engineering.

EXPERIMENTAL

Materials

Hydroxypropyl starch (HPS) (molecular weight $<2 \times 10^6$ Da and substitution degree <7%), PEO ($M_V = 9 \times 10^5$ Da, Sigma-Aldrich), poly(methyl methacrylate) (PMMA) ($M_W = 12 \times 10^5$ Da, Sigma-Aldrich), and chloroform (Panreac) were used as received.

For biological assays, Thermanox® (TMX) discs were supplied by Labclinics S. L. and polypropylene tubes were purchased from Sarstedt. Tissue culture media, additives, trypsin, 3-(4,5-dimethylthiazol-2-yl)-2,5 diphenyltetrazolium bromide (MTT), Triton X-100, and phosphate buffered solution (PBS) of pH 7.4 were all supplied by Sigma-Aldrich, foetal bovine serum (FBS) was purchased from Gibco and the Alamar Blue reagent from Serotec.

Electrospinning Process

HPS and PEO powders were accurately weighed and mixed to obtain blends with HPS/PEO ratios of 30 : 70, 50 : 50, 60 : 40, 70 : 30, 80 : 20, and 90 : 10 wt %. Each powder mixture was dissolved in bidistilled water (10 wt %). For the complete dissolution of HPS heating to boiling point was required.

The corresponding polymer solution was placed into a syringe with an 18-gauge blunt-end needle that was mounted in a syringe pump (Cole-Parmer). Randomly oriented nanofibers were electrospun by applying a voltage of 11–14 kV using a Spellman CZE1000R high voltage supply (0–30 kV CZE1000R; Spellman High Voltage Electronics Corp.) with a low current output limited to a few μA. The ground plate (stainless steel sheet on a screen) was placed at 30 cm from the needle tip. The flow rate of the polymer solution ranged between 0.02 and 0.04 mL/h depending on the sample. The resulting fibres were collected on the screen to produce a sheet of nonwoven fabric. Electrospinning conditions applied for each sample are shown in Table I. As both HPS and PEO components are highly hydrophilic, the mats of HPS/PEO were coated with PMMA to improve their water stability. Mats were immersed in a chloroform solution (1 wt %) of PMMA, extracted, and left to dry in air until constant weight.

Characterization of the Electrospun Mats

The Fourier transform infrared (FTIR) analysis of the electrospun samples was performed in a Nicolet Magna-IR 560 spectrometer with an attenuated total reflectance (ATR) objective equipped with a zinc selenide crystal (Spectra Tech.). The spectra were collected at a spectral resolution of 8 cm^{-1} by accumulating 64 scans.

The thermal stability of the electrospun samples was evaluated by thermogravimetric analysis (TGA) using a TGA Q500 (TA instruments) apparatus. Thermograms were recorded at a

Table I. Electrospinning Conditions for Different HPS/PEO Blends

HPS/PEO (wt %)	Distance to collector, *d* (cm)	Flow, *f* (mL/h)	Voltage, *V* (kV)
30 : 70	30	0.02	14
50 : 50	30	0.02	13
60 : 40	30	0.02	11
70 : 30	30	0.02	11
80 : 20	30	0.04	11
90 : 10	30	0.04	11

heating rate of 10°C/min under a nitrogen atmosphere, in a range of 40–700°C.

The morphology of electrospun mats was studied by scanning electron microscopy (SEM) using a SEM-Hitachi-S-2700 equipment at an accelerating voltage of 15 keV. Samples were coated with an 8 nm Pt/Au layer to reduce electron charging effects. Fiber diameters were determined by measuring random fibers of different experiments for each blend composition. In each case, a minimum of 130 fibers was chosen to obtain an average value with standard deviation between 40 and 100 nm.

In Vitro Degradation of Electrospun Mats

The degradation of the PMMA-coated mats (14-mm diameter and 3-mm thickness) was evaluated in a PBS of pH = 7.4 at 37°C. The mats were accurately measured and weighed, and then introduced into 10 mL of PBS. At different time intervals the samples were removed and transferred to an oven at 50°C where they were kept until they reached a constant weight. The weight loss was calculated from the following equation:

$$\%\ \text{Weight loss} = [(W_o - W_s)/W_o] \times 100$$

where W_s is the weight of the dried sample degraded at time t and W_o is the initial weight of the dry specimen. In all the experiments, a minimum of three samples were measured and averages were recorded.

After the test, infrared analysis of the samples was performed to examine the variations in their structure. Morphology of the fibers was also observed by SEM.

Cellular Behavior

The biological response of the materials was tested using fibroblasts of human adult skin (HFB, Innoprot). The culture medium was Dulbecco's modified Eagle's medium enriched with 4500 mg/mL of glucose (DMEM) supplemented with 10% foetal bovine serum (FBS), 200 m*M* L-glutamine, 100 units/mL penicillin, and 100 μg/mL streptomycin, modified with HEPES. The culture medium was changed at selected time intervals with great care to cause minimum disturbance to culture conditions. TMX was used as a negative control and a 1% (v/v) Triton X-100 solution (Triton) was used as a positive control.

Coated mats (14-mm diameter and 3-mm thickness) of HPS/PEO mixtures in 70 : 30 and 80 : 20 wt % proportions were tested in direct and indirect experiments. All specimens were sterilized using an ultraviolet lamp (HNS OSRAM, 263 nm, 3.6 UVC/W) for 2 h.

Cytotoxicity of Mats

Samples of mats and TMX were set up in 5 mL of DMEM, FBS-free. They were placed on a roller mixer at 37°C and the medium was removed at different time periods (1, 2, and 7 days) and replaced with other 5 mL of fresh medium. All the extracts were obtained under sterile conditions. HFB were seeded in complete medium at a density of 8×10^4 cells/mL in a sterile 96-well culture plate and incubated to confluence. After 24 h of incubation, the medium was replaced with the corresponding test extracts and extracts coming from TMX discs and a Triton solution in culture medium, and, then incubated at 37°C in humidified air with 5% CO_2 for 24 h. A solution of MTT was prepared in warm PBS (0.5 mg/mL) and the plates were incubated at 37°C for 4 h. Excess medium and MTT were removed and DMSO was added to all wells to dissolve the MTT taken up by the cells. This was mixed for 10 min and the absorbance was measured with a Biotek Synergy HT detector using a test wavelength of 570 nm and a reference wavelength of 630 nm. The cell viability was calculated according to the following equation:

$$\text{Cell viability} = 100 \times (\text{OD}_S - \text{OD}_B)/(\text{OD}_C - \text{OD}_B)$$

where OD_S, OD_B, and OD_C are the optical density of formazan production for the sample (S), blank (B) (culture medium without cells), and control (C), respectively. Analysis of variance (ANOVA) of the results for mats was performed with respect to TMX at $P < 0.05$ of significance level.

Cell Adhesion and Proliferation

Alamar Blue Assay. HFB cells were seeded at a density of 14×10^4 cells/mL for 24 h over the testing dry specimens placed in 24-well culture plate. Next, 2 mL of Alamar Blue dye (10% Alamar Blue solution in phenol red-free DMEM medium) was added to each specimen. After 4 h of incubation 100 mL ($n = 4$) of culture medium for each test sample was transferred to a 96-well plate, and the fluorescence emission was measured at 570 nm with a Biotek Synergy HT detector. The specimens were washed with PBS twice to remove all residue of the reagent, and 1 mL of culture medium was added to monitor the cells over the materials. This step was carried out on days 1, 4, 7, and 14. ANOVA of the results for mats was carried out with respect to TMX at $P < 0.05$ of significant level.

Scanning Electron Microscopy. The materials were placed in a 24-well plate (in duplicate) and seeded with HFB at a density of 14×10^5 cells/mL. These were incubated at 37°C for 1, 2, and 7 days. After each period of time, the cells were fixed with 2.5% glutaraldehyde buffered in distilled water for 24 h at room temperature and then washed and dried. The dried samples were sputter-coated with Au/Pd (80/20) before examination under a SEM apparatus (Philips XL 30) at an accelerating voltage of 25 KeV.

RESULTS AND DISCUSSION

Characterization of Electrospun Mats

As shown in the SEM images displayed in Figure 1, uniform fibers were obtained in all the varying HPS/PEO blends except for the

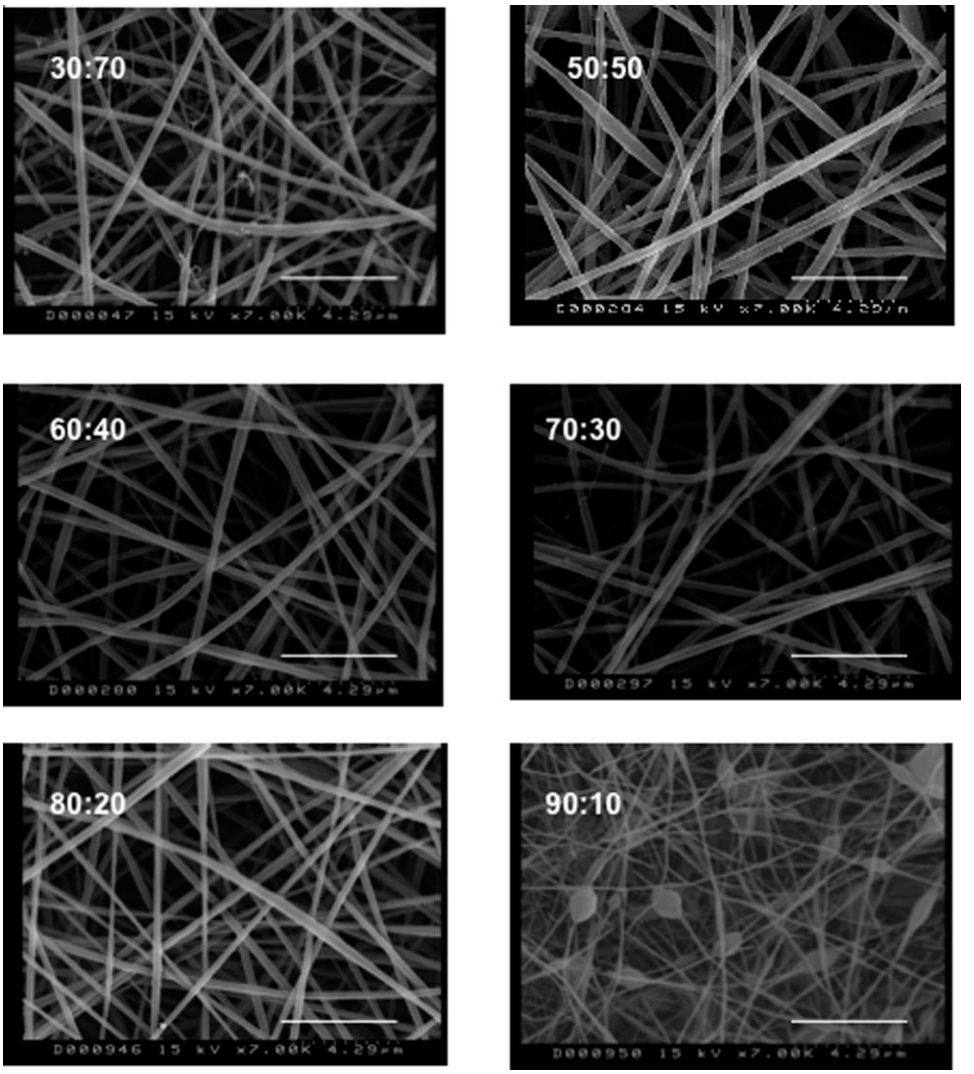

Figure 1. Scanning electron micrographs of electrospun HPS/PEO mixtures in different proportions, 30 : 70, 50 : 50, 60 : 40, 70 : 30, 80 : 20, and 90 : 10 respectively. Scale bars indicate 4.29 μm.

90 : 10 mixture, for which the presence of drops appeared. This fact indicates that neither viscosity nor consistency of this blend solution were adequate to be electrospun. In addition to observing the morphology of the fibers, average fiber diameters were determined from the SEM images. Results for the different HPS/PEO blends are shown in Table II. Diameters of fibres were found to be homogeneous and displayed average values in a narrow range independent of the blend proportion except for the 90 : 10 blend for which the fiber diameters were smaller, probably due to the fact that this blend ratio produces a mixture of fibers and drops. Thus, mats of fibers with average diameters around 300 nm were successfully obtained for HPS/PEO ratios between 30 : 70 and 80 : 20, i.e., electrospun fibers containing high starch content, i.e., 80 wt % HPS, could be processed. This proportion is even higher than that reported in the existing literature on starch.[20–24] Therefore, to have mats of nanofibers to be used as scaffolds in tissue engineering applications, the blends with the highest polysaccharide content, i.e., HPS/PEO 70 : 30 and 80 : 20 were selected for further work.

Mats obtained from the water solution present an obvious hydrophilicity. Consequently, sticky and delicate mats difficult to handle were obtained. To improve stability and mechanical properties, electrospun mats of HPS/PEO blends were coated with PMMA and their morphology examined by SEM. As it can be observed in Figure 2, coated fibres retained their fibrous morphology. Table III shows the average diameter values of

Table II. Values of Average Diameter of the Fibers Obtained from HPS/PEO Mixtures in Different Proportions

HPS/PEO (wt %)	Fiber average diameter (nm)
30 : 70	286 ± 90
50 : 50	281 ± 87
60 : 40	334 ± 54
70 : 30	324 ± 91
80 : 20	303 ± 55
90 : 10	143 ± 42

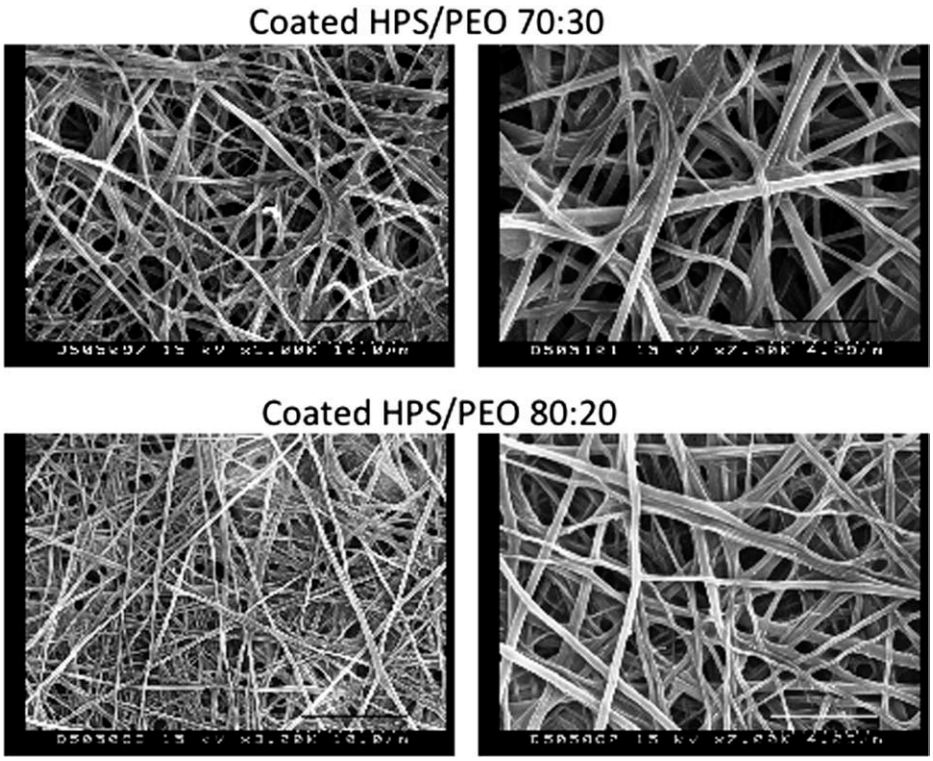

Figure 2. Scanning electron micrographs of PMMA-coated electrospun HPS/PEO mixtures in 70 : 30 and 80 : 20 proportions. Scale bars indicate 10 μm (right) and 4.29 μm (left).

coated fibers obtained from the HPS/PEO 70 : 30 and 80 : 20 mixtures along with those of uncoated ones. Looking at the data, it is clear that the average diameters of the fibers do not significantly ($P < 0.05$) vary after coating with PMMA. This indicates the extreme thinness of the coating. However, it is still enough to be able to stabilize the mat.

Coated and uncoated fibers underwent thermal and structural characterization using TGA and ATR-FTIR techniques. Figure 3 shows the derivative thermogravimetric curves (DTG) for the uncoated and coated samples along with those of pure HPS, PEO, and PMMA. The DTG curves for the pure HPS and PEO [Figure 3(a)] indicated a single stage of weight loss up to ca. 330°C for HPS and 400°C for PEO. A loss of weight in the range 310–358°C has been ascribed in the literature to the thermal degradation of amylose and amylopectin in starch samples,[32] which involves dehydration and depolymerization as the two main processes associated with the degradation mechanism. Thermal degradation of PEO occurring in a single step is ascribed to a concerted radical mechanism initiated by random scission of C—O and C—C bonds in the polymer chains.[33–34]

Table III. Values of Average Diameter of the Uncoated and Coated Fibers Obtained from HPS/PEO Mixtures in Different Proportions

	Average diameter (nm)	
HPS/POE (wt %)	Uncoated fibers	Coated fibers
70 : 30	324 ± 91	321 ± 69
80 : 20	303 ± 55	297 ± 87

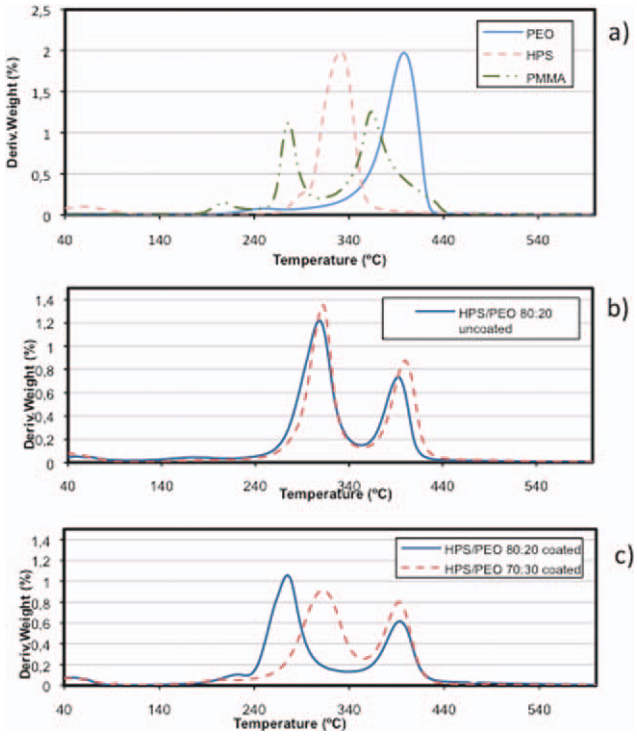

Figure 3. Thermogravimetric curves of the derivative weight loss versus temperature (DTG) for the pure HPS, PEO, and PMMA (a), uncoated samples of HPS/PEO mixtures in 70 : 30 and 80 : 20 proportions (b), and coated samples of same composition (c). [Color figure can be viewed in the online issue, which is available at wileyonlinelibrary.com.]

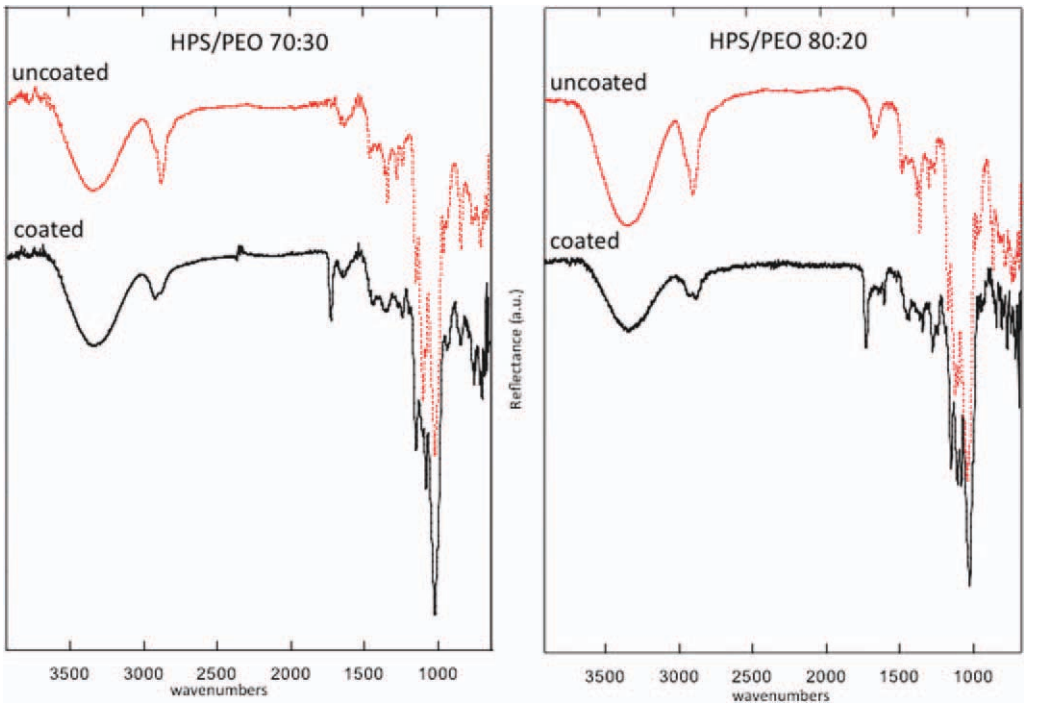

Figure 4. ATR-FTIR spectra of the coated and uncoated samples of HPS/PEO mixtures in 70 : 30 and 80 : 20 proportions. [Color figure can be viewed in the online issue, which is available at wileyonlinelibrary.com.]

Pure PMMA, on the other hand, underwent thermal degradation in two main stages [Figure 3(a)], the first one, up to ca. 276°C, has been attributed to the decomposition of vinylidene end groups[35] and the second and main one, up to ca. 365°C, to random scission of main chains. In addition a first loss weight at ca. 207°C is shown which has been attributed to the sterically hindered head to head linkages.[36] The DTG curves for the uncoated fibers [Figure 3(b)] show two main stages of weight loss, the first one at a temperature around 312°C which can be attributed to the main decomposition stage of the HPS. The second peak at a temperature of 400°C coincides with the temperature of the main weight loss stage of the pure PEO. The DTG curves of the coated samples [Figure 3(c)] show two main peaks for both mixtures the first one in the range 280–300°C that could be attributed to HPS and also to the vinylidene decomposition of end groups of PMMA[35] and the second peak ca. 390°C that could be due to the main weight loss of PEO and the random scission of the main chains of PMMA.

Turning now to the structural characterization of the fibers, Figure 4 shows the ATR-FTIR spectra for uncoated and coated samples. The spectra of the uncoated samples show the bands typical of carbohydrate such as the undefined broad band at over 3500 cm^{-1} resulting from the stretching vibration of OH groups. Similarly bands in the region of 1550–1350 cm^{-1} due to the deformation vibration of the methylene groups and bands in the region of 1350–1050 cm^{-1} due to the stretching vibration of ether groups can be observed. In addition to these carbohydrate bands, the most characteristic band for PEO, namely the C—O—C stretching band of the ether group at 1100 cm^{-1}, is present. In the ATR-FTIR spectra of coated samples, besides the bands corresponding to the HPS and PEO polymers the band representing the carbonyl stretching vibration of PMMA at 1730 cm^{-1} appears, confirming the presence of the three components in the coated fibers.

In Vitro Degradation

Figure 5 shows the degradation curves of the coated mats after 1 month's immersion in PBS of pH = 7.4 at 37°C. The weight loss experienced by the HPS/PEO 70 : 30 sample was slightly higher than that observed for the 80 : 20 blend, due to the higher PEO content that is dissolved firstly in the aqueous medium. In neither of the two cases a weight loss exceeding 50 wt % was observed.

The changes in the chemical structure of the mats throughout the degradation process were monitored using ATR-FTIR

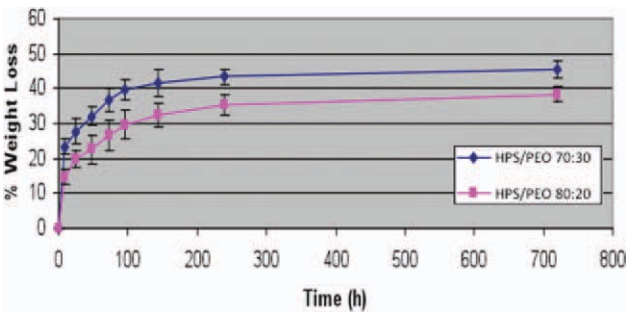

Figure 5. Degradation curves of coated mats of HPS/PEO mixtures in 70 : 30 and 80 : 20 proportions in phosphate buffer solution (PBS) of pH 7.4 at 37°C. [Color figure can be viewed in the online issue, which is available at wileyonlinelibrary.com.]

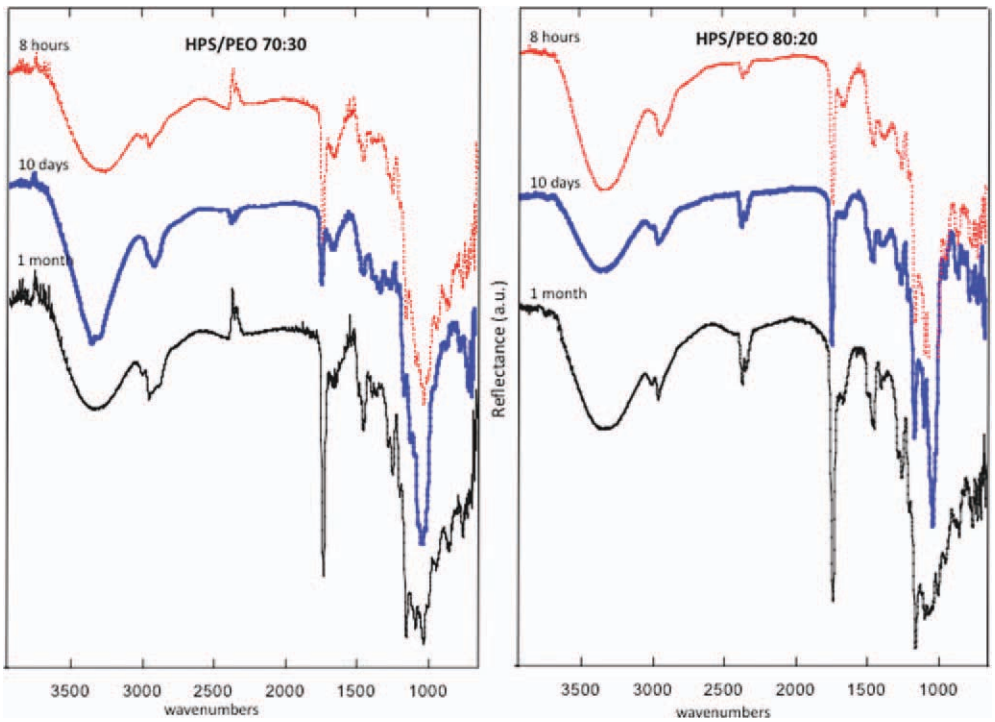

Figure 6. ATR–FTIR spectra for HPS/PEO 70 : 30 and 80 : 20 samples after 8 h, 10 days and 1 month of degradation in PBS. [Color figure can be viewed in the online issue, which is available at wileyonlinelibrary.com.]

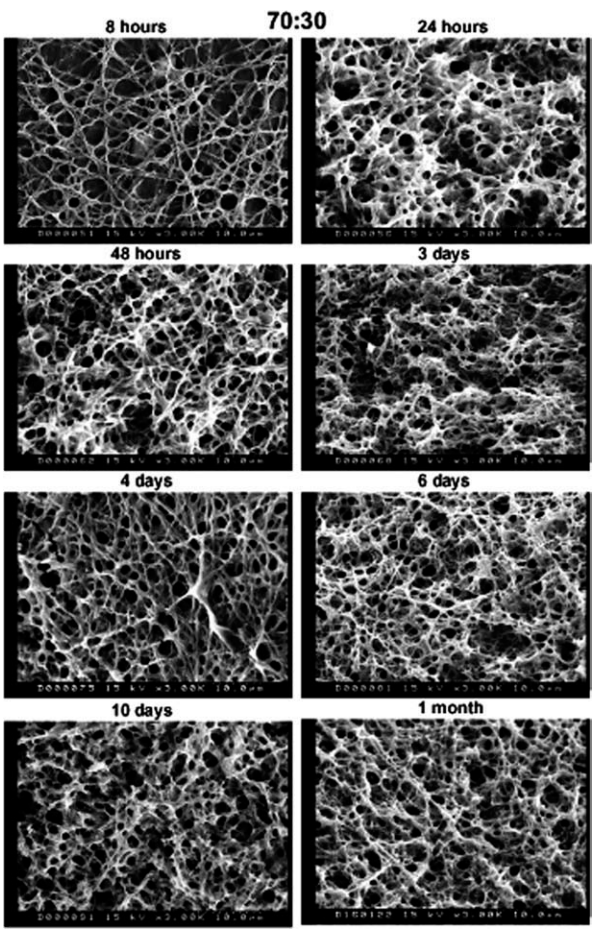

Figure 7. SEM images of mats of HPS/PEO 70 : 30 at different degradation periods in PBS. Scale bars indicate 10 μm.

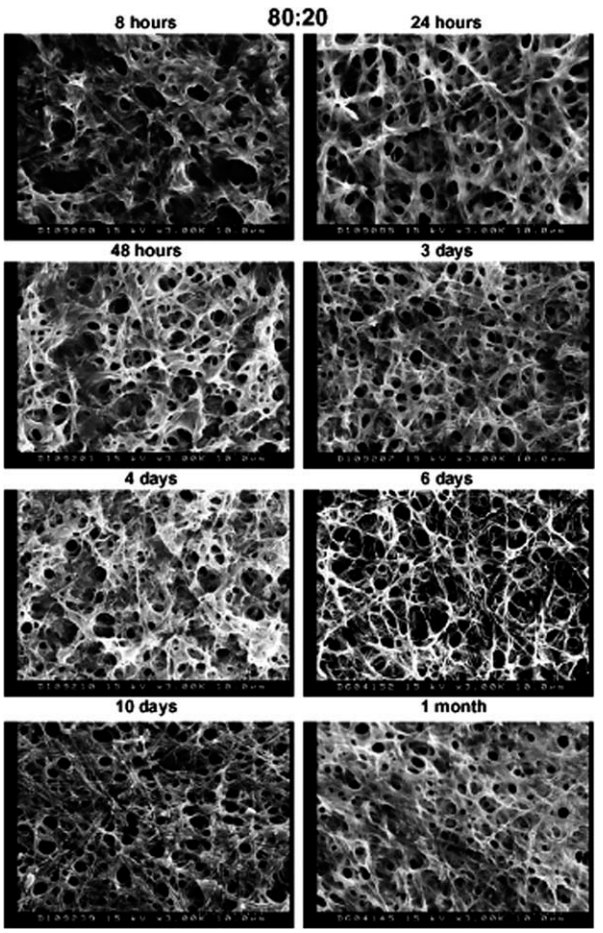

Figure 8. SEM images of mats of HPS/PEO 80 : 20 at different degradation periods in PBS. Scale bars indicate 10 μm.

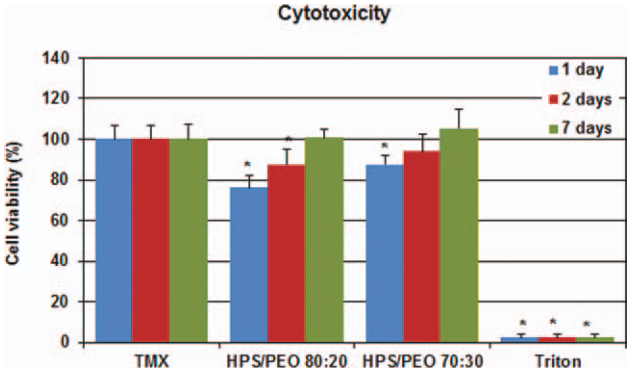

Figure 9. MTT assay results for coated mats of HPS/PEO 70 : 30 and 80 : 20 and for the negative and positive controls TMX and Triton, respectively. All the results are shown as mean ± S.D. asterisk (*) depicts a significant difference between results of the corresponding sample with respect to TMX ($P < 0.05$). [Color figure can be viewed in the online issue, which is available at wileyonlinelibrary.com.]

spectroscopy. Also, the morphology of the degraded samples with time of immersion was examined by SEM. Figure 6 shows the ATR-FTIR spectra for HPS/PEO samples after 8 h, 10 days and 1 month of degradation. As the test progresses the PEO characteristic band at 1100 cm^{-1} shows a decrease due to increasing dissolution of this polymer in the medium. However, the PMMA band at 1730 cm^{-1} becomes more intense as a consequence of the weight loss of the sample at expense of the hydrophilic polymer. The variation in the intensities of both bands is more noticeable in the spectra of the samples that have been immersed for 1 month.

Looking at the modifications observed in the morphology of the fibers with soaking time (Figures 7 and 8), it is evident that both blends retain their fiber structure even after a month. The measurements of the diameter of fibers after the degradation test could not be carried out because the samples underwent a partial loss of weight, resulting in a material with porous structure. Nevertheless, it is clear that these coated mats were able to retain their fiber structure practically intact for at least 1 month's immersion in PBS. This degradation pattern supports the application of these mats as scaffolds in tissue engineering.

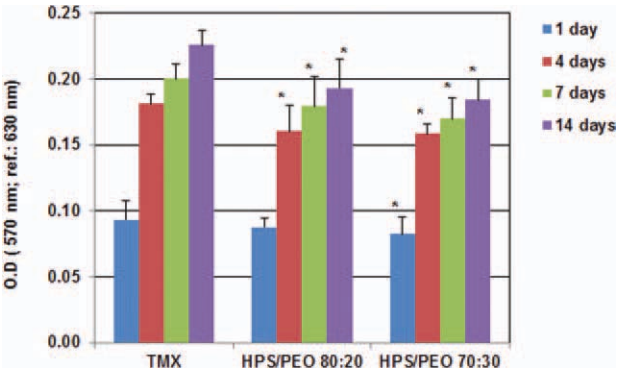

Figure 10. Alamar Blue assay results for coated mats of HPS/PEO 70 : 30 and 80 : 20 and for the negative control TMX. All the results are shown as mean ± S.D. asterisk (*) depicts a significant difference between the corresponding sample with respect to TMX ($P < 0.05$). [Color figure can be viewed in the online issue, which is available at wileyonlinelibrary.com.]

Biological Behavior

The level of toxicity of the fibrous mats toward HFB was evaluated using an ISO10993-5 standard method of indirect MTT assay.[37] Figure 9 shows the cellular response in the presence of the extracts lixiviated from the coated scaffolds in culture

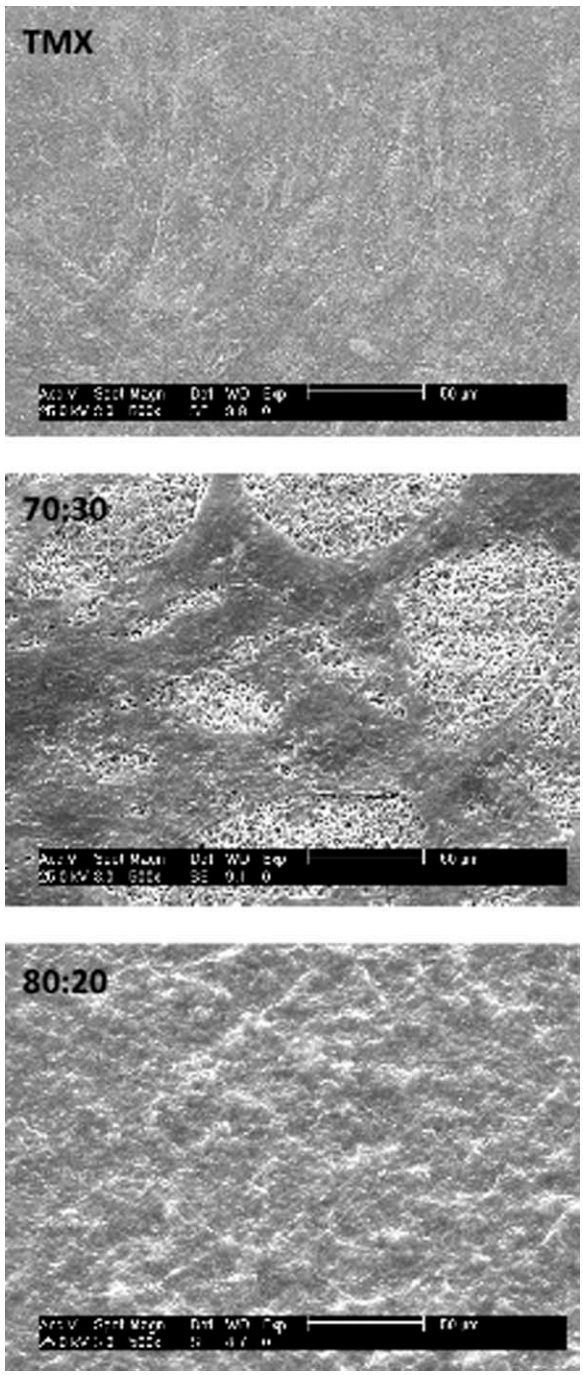

Figure 11. SEM images of the colonization of HFB on TMX and mats of HPS/PEO 70 : 30 and 80 : 20 after 7 days of seeding. Scale bars indicate 50 μm.

medium at different times. Cell viability significantly decreased in the presence of the extracts of both HPS/PEO blends taken at 1 and 2 days, however, cell viability was higher than 75% in all cases and cytotoxicity of mats of both blends was not compromised.[37] Moreover, cell viability recovered for extracts of both composition mats taken at longer times, reaching values of 100% when cells were incubated with the lixiviates of 7 days, the results showing no significant differences with respect to the TMX control.

Adhesion and proliferation of cells seeded on scaffolds is an essential requirement to generate a tissue-like structure. Therefore, the ability of fibroblasts to adhere and growth on the coated electrospun mats of HPS/PEO blends was examined. Figure 10 shows the percentage of viable cells on the samples at different days of testing. Both HPS/PEO 70 : 30 and 80 : 20 mats showed adhesion and proliferation patterns similar to that of TMX control, with comparable percentage of adhered cells at 1 day for the blend of HPS/PEO 80 : 20 and significantly low percentage for the blend HPS/PEO 70 : 30. Afterward, significantly lower proliferation on both scaffolds between days 4 and 14 was observed. However, the overall results indicate that these systems are able to support the colonization and growth of human fibroblasts on their surfaces. To illustrate this result, SEM analysis of the cultured mats was performed and the microphotographs taken after 7 days of seeding are shown in Figure 11. It is clear that good colonization was achieved on both types of samples compared with the TMX control, being higher on the sample with higher polysaccharide content.

CONCLUSIONS

HPS, a well known biodegradable water-soluble polymer, was successfully electrospun into nanofibers by adding different amounts of PEO (between 20 and 70 wt %). Thus, a novel aspect of this work is that very high starch content (up to 80 wt %) nanofibers based on HPS were produced with success. This is an encouraging result because of the difficulty of starch in being processed by the electrospinning technique which is reflected in the scare literature reported regarding this type of material.

The stability of the HPS rich mats (70 and 80 wt %) in physiological fluid was improved by applying a thin coating of PMMA, achieving that weight loss underwent by mats in any of the cases never exceeded 50 wt % after 1 month of immersion. Moreover, the degradation of the mats produced a porous architecture while retaining their fiber structure at the end of the experiment.

Cell culture assays showed that mats with high contents of HPS were not cytotoxic against human fibroblast and cells were able to adhere and proliferate on the fibrous materials following growth patterns comparable with that of tissue culture plastic control.

In summary, the overall findings on the degradation pattern and biological response of HPS rich mats support their great potential to be used as scaffolds in tissue engineering applications.

ACKNOWLEDGMENTS

The financial support has been granted by Ministry of Science and Innovation through the project MAT2010-18155 and by the University of the Basque Country (UPV) with "University of the Basque Country group grants." M. Fernández-Gutiérrrez also thanks to the JAE-doc program of CSIC.

REFERENCES

1. Still, T. J.; Von Recum, H. A. *Biomaterials* **2008,** *29*, 1989.
2. Greiner, A.; Wendorff, J. H. *Angew. Chem. Int. Ed.* **2007,** *46*, 5670.
3. Li, D.; Xia, Y. N. *Adv. Mater.* **2004,** *16*, 1151.
4. Zhong, S.; Teo, W. E.; Zhu, X.; Beuerman, R.; Ramakrishna, S.; Yung, L. Y. L. *Biomacromolecules* **2005,** *6*, 2998.
5. Huang, Z. M.; Zhang, Y. Z.; Kotaki, M.; Ramakrishna, S. *Compos. Sci. Technol.* **2003,** *63*, 2223.
6. Li, W. J.; Laurencin, C. T.; Caterson, E. J.; Tuan, R. S.; Ko, F. K. *J. Biomed. Mater. Res.* **2002,** *60*, 613.
7. Agarwal, S.; Wendorff, J. H.; Greiner, A. *Adv. Mater.* **2009,** *21*, 3343.
8. Liu, Y.; Ji, Y.; Ghosh, K.; Clark, R. A. F.; Huang, L.; Rafailovich, M. H. *J. Biomed. Mater. Res. A* **2008,** *87A*, 1092.
9. Cui, W.; Zhu, X.; Yang, Y.; Li, X.; Jin, Y. *Mat. Sci. Eng. C-Mater.* **2009,** *29*, 1869.
10. Thorvaldsson, A.; Stenhamre, H.; Gatenholm, P.; Walkenström, P. *Biomacromolecules* **2008,** *9*, 1044.
11. Gomes, M. E.; Holtorf, H. L.; Reis, R. L.; Mikos, A. G. *Tissue Eng.* **2006,** *12*, 801.
12. Holtorf, H. L.; Datta, N.; Jansen, J. A.; Mikos, A. G. *J. Biomed. Mater. Res. A* **2005,** *74A*, 171.
13. Mygind, T.; Stiehler, M.; Baatrup, A.; Li, H.; Zou, X.; Flyvbjerg, A.; Kassem, M.; Bünger, C. *Biomaterials* **2007,** *28*, 1036.
14. Heydarkhan-Haguall, S.; Schenke-Layland, K.; Dhanasopon, A. P.; Rofail, F. Smith, H.; Wu, B. M.; Shemin, R.; Beygui, R. E.; Maclellan, W. R. *Biomaterials* **2008,** *29*, 2904.
15. Hutmacher, D. W.; Schantz, J. T.; Lam, C. X. *J. Tissue Eng. Regen. Med.* **2007,** *1*, 245.
16. Lutolf, M. P.; Hubbell, J. A. *Nat. Biotechnol.* **2005,** *23*, 47.
17. Lou, C. W.; Lin, J. H.; Yen, K. C.; Lu, C. T.; Lee, C. Y. *Text. Res. J.* **2008,** *78*, 254.
18. Jeong, S. I.; Lee, A. Y.; Lee, Y. M.; Shin, H. *J. Biomater. Sci. Polym. Ed.* **2008,** *19*, 339.
19. Jin, H. J.; Fridrikh, S. V.; Rutledge, G. C.; Kaplan, D. L. *Biomacromolecules* **2002,** *3*, 1233.
20. Uyar, T.; Besenbacher, F. *Eur. Polym. J.* **2009,** *45*, 1032.
21. Rujitanaroj, P. O.; Pimpha, N.; Supaphol, P. *Polymer* **2008,** *49*, 4723.
22. Xu, S.; Li, J.; He, A.; Liu, W.; Jiang, X.; Zheng, J.; Han, C. C.; Hsiao, B. S.; Chu, B.; Fang, D. *Polymer* **2009,** *50*, 3762.
23. Shalumon, K. T.; Binulal, N. S.; Selvamurugan, N.; Nair, S. V.; Menon, D.; Furuike, T.; Tamura, H.; Jayakumar R. *Carbohydr. Polym.* **2009,** *77*, 863.

24. Lee, K.Y.; Jeong, L.; Kang Y. O.; Lee, S. J.; Park, W. H. *Adv. Drug Deliv. Rev.* **2009,** *61*, 1020.
25. Martins, A.; Chung, S.; Pedro, A. J.; Sousa, R. A.; Marques, A. P.; Reis, R. L.; Neves N. M. *J. Tissue Eng. Regen. Med.* **2009,** *3*, 37.
26. Alves da Silva, M.; Crawford, A.; Mundy, J.; Martins, A.; Araujo, J. V.; Hatton, P. V.; Reis, R. L.; Neves, N. M. *Tissue Eng. Part. A* **2002,** *15*, 377.
27. Jukola, H.; Nikkola, L.; Gomes, M. E.; Reis, R. L.; Asham-makhi, N. *AIP Conf. Proc.* **2008,** *973*, 971.
28. Tuzlakoglu, K.; Bolgen, N.; Salgado, A. J.; Gomes, M. E. *J. Mater. Sci. Mater. Med.* **2005,** *16*, 1099.
29. Gomes, M. E.; Godinho, J. S.; Tchalamov, A. M.; Cunha, A. M.; Reis, R. L. *Mat. Sci. Eng. C-Mater.* **2002,** *20*, 19.
30. Adomaviciute, E.; Milasius, R.; Zemaitaitis, A.; Bendorai-tiene, J.; Leskovsek, M.; Demsar, A. *Fibres Tex. East Eur.* **2009,** *17*, 29.
31. Weijie, X.; Wen, Y.; Yiqi, Y. *Biotechnol. Prog.* **2009,** *25*, 1788.
32. Canché-Escamilla, G.; Canché-Canché, M.; Duarte-Aranda, S.; Cáceres-Farfán, M.; Borges-Argaez R. *Carbohyd. Polym.* **2011,** *86*, 1501.
33. Grassie, N.; Perdomo Mendoza, A. *Polym. Degrad. Stab.* **1985,** *9*, 155.
34. Pielichowski, K.; Flejtuch, K. *J. Anal. Appl. Pyrol.* **2005,** *73*, 131.
35. Kashiwagi, T.; Inaba, A.; Brown, J. E.; Hatada, K.; Kitayama, T.; Masuda E. *Macromolecules* **1986,** *19*, 2160.
36. Arshad, M.; Masud, K.; Arif, M.; Rehman, S.; Arif, M.; Zaidi, J. H.; Chohan, Z. H.; Saeed, A.; Qureshi, A. H. *J. Therm. Anal. Calorim.* **2009,** *96*, 873.
37. ISO10993-5. Biological evaluation of medical devices—Part 5: Tests for in vitro cytotoxicity (**2009**).